Ca and Pr substitution in Y- and Sm-based 1:2:3 compounds

M. Andersson and Ö. Rapp
Solid State Physics, The Royal Institute of Technology, S-100 44 Stockholm, Sweden

T. L. Wen, Z. Hegedüs, and M. Nygren
Inorganic Chemistry, Arrhenius Laboratory, Stockholm University, S-104 05 Stockholm, Sweden
(Received 10 August 1992; revised manuscript received 26 April 1993)

Substitution with equal amounts of Ca and Pr has been studied mainly in Y- and Sm-based 1:2:3 samples and with some results also for Nd-based samples. Structural and chemical analysis and measurements of the superconducting T_c and the upper critical magnetic field were performed. It was found that Ca and Pr can be dissolved in the orthorhombic structure up to about 25 at. % each in both Y- and Sm-based samples while for larger concentrations, only Pr continued to enter into the 1:2:3 structure. The depression of T_c with Ca-Pr doping was found to be linear in concentration in contrast to the accelerated decrease in samples doped with only Pr. The rate of depression of T_c increased in the sequence Y-, Sm-, and Nd-based hosts. The results suggest that Ca-Pr doping isolates a characteristic Pr-impurity effect in 1:2:3 samples. The critical magnetic-field slopes of Y- and Sm-based samples were almost independent of Ca-Pr content in the cosolubility region while a strong decrease was observed for larger Pr content, similar to 1:2:3 samples doped with Pr only. These results suggest an almost-temperature-independent magnetic pair-breaking effect by Pr.

I. INTRODUCTION

The monotonic decrease of T_c with increasing Pr concentration in the orthorhombic phase of $YBa_2Cu_3O_{7-\delta}$ is unique among the $4f$ elemental substitutions in this compound. A large number of investigations by different methods have been made in order to explain this result,[1] with the underlying idea that understanding the exception would help clarify the nature of superconductivity in the 1:2:3 compounds.

However, there is no agreement on the interpretation of these results. Explanations include Pr hole contribution, Pr $4f$ shell hybridization with the Cu-O plane, and magnetic pair breaking by Pr ions. Magnetic susceptibility,[2,3] muon-spin relaxation,[4,5] Hall effect,[6] and specific-heat measurements,[7,8] have suggested that Pr has a valence larger than $+3$, and therefore contributes electrons which destroy holes in the Cu-O plane. On the other hand high-energy spectroscopy[9,10] and optical investigations[11] have indicated the presence of trivalent Pr. The depression of T_c with Pr concentration could then be due to magnetic pair breaking. This has been suggested[3,12] by the similarity of the T_c vs impurity concentration curve to the prediction from Abrikosov-Gorkov (AG) theory,[13] and by further results form the critical magnetic field.[12] On the other hand, recent work has indicated that the T_c vs Pr concentration curve is not AG-like.[14] Further work has also suggested that the low-temperature anomalous $H_{c2}(T)$ previously observed,[12] possibly was a spurious effect.[15] Additional support for magnetic pair breaking has been obtained from spin-polarized band-structure calculations.[16] The large ionic radius of the Pr ion could possibly explain the larger sensitivity of the Pr moment, as compared to the other rare-earth substitutions.

The suggestion that Pr may cause a mobile hole to become localized[17] may offer a reconciliation between these different points of views. Such localization has been claimed from photoemission and polarized Raman scattering,[18,19] and from Ce substitution of Y-based thin films obtained by laser ablation.[20]

In a study of $YBa_2Cu_3O_{7-\delta}$ doped with different amounts of Ca and/or Pr, Neumeier *et al.*[21] found that the effect of Pr doping could be described as a combination of both effects mentioned: a destruction of about one mobile hole per Pr atom and a magnetic pair-breaking effect with an initial depression of about 1 K/at.% Pr. A similar analysis was recently used in an investigation of the isotope effect of $YBa_2Cu_3O_{7-\delta}$ doped with different amounts of Ca and/or Pr, with similar results.[22] Although the nature of hole destruction is not clarified by such analysis, it clearly represents a useful empirical summary of experimental T_c data.

According to the results of Ref. 21, doping with about equal amounts of Ca and Pr would compensate for the change of mobile charge carriers due to the Pr addition. We have used this result in order to try to isolate magnetic pair breaking in 1:2:3 compounds, and report here on the results of doping with Ca and Pr in equal proportions in different hosts, i.e., Y- and Sm-based 1:2:3 compounds. Some results from Nd-based 1:2:3 compounds are also included. Part of this work has been reported previously in short communications.[23,24] Different hosts give additional possibilities to test the different models of the Pr effect. In particular, since the Sm^{3+} and Nd^{3+} ions are larger than Y^{3+}, the overlap between wave functions in the Cu-O plane and on the Y position would vary for different hosts, and one can investigate if this is correlated with a variation of magnetic pair breaking. Similar ideas have

been used recently in studies of Pr doping in several different rare-earth 1:2:3 compounds.[25–27] In those cases only Pr was doped into the 1:2:3 superconductors, and the separation of different effects of Pr is less clear.

In this paper we report on structural studies and measurements of T_c and upper critical magnetic field of $Y_{1-2x}Ca_xPr_xBa_2Cu_3O_{7-\delta}$, $Sm_{1-2x}Ca_xPr_xBa_2Cu_3O_{7-\delta}$, and $Sm_{1-x}Pr_xBa_2Cu_3O_{7-\delta}$, and some T_c results for $Nd_{1-2x}Ca_xPr_xBa_2Cu_3O_{7-\delta}$. The results for Ca-Pr doping in different hosts are similar, with somewhat stronger concentration dependence of T_c and of critical-field slopes for the larger ions. In particular, it is found that equal amounts of Ca and Pr can be dissolved in the orthorhombic phase only up to about $x=0.25$ for both Y- and Sm-based hosts, and that beyond that only the Pr concentration increases. The slopes of the critical-field curves are found to be almost constant or to increase lightly with Ca-Pr doping for $x<0.25$ in both these systems, while for $x>0.25$ the critical-field slope decreases at a rate comparable to that observed for Pr-only-doped Sm- or Y-based 1:2:3 compounds. This result would suggest that if the depression is due to magnetic pair breaking, such pair breaking is close to being temperature independent, i.e., AG-like.

II. SAMPLE PREPARATION

The samples were prepared by a standard powder-synthesis technique from the appropriate amounts of CuO, Y_2O_3, Sm_2O_3, Nd_2O_3, Pr_6O_{11}, $CaCO_3$, and $BaCO_3$. The oxygen content of the starting materials was determined by thermogravimetric analysis.

All samples were prepared by a similar route. After careful mixing, the powders were compacted to cylindrical tablets and subjected to a first heat treatment, crushed, reground, and sintered a second time. Finally the samples were annealed in oxygen. Time and temperature for each heat treatment are listed in Table I. For Ca-Pr doping in Y-based 1:2:3 compounds, two series were prepared, using slightly different preparation conditions. For sample series 2 and for the Nd-based Ca-Pr doping, only x-ray investigations and T_c measurements were made.

III. STRUCTURAL PROPERTIES

A. Techniques

The samples were characterized by their x-ray-powder-diffraction patterns obtained at room temperature in a Guinier-Hägg focusing camera using Cu$K\alpha$ radiation and Si as an internal standard. The evaluation of photographs was performed with a microsdensitometer system.[28] The amount of $BaCuO_2$ impurities was estimated from the ratio of the intensities of the strongest reflections from the 1:2:3 phase and of the impurity phase.

TABLE I. Sample preparation conditions.

Sample series	First heat treatment (air)	Second heat treatment (air)	Heat treatment in oxygen
Y-Ca-Pr 1	920 °C, 24 h	950 °C, 48 h	450 °C, 48 h
Y-Ca-Pr 2	910 °C, 24 h	950 °C, 24 h	450 °C, 24 h
Nd-Ca-Pr	910 °C, 24 h	930 °C, 24 h	450 °C, 24 h
Sm-Ca-Pr	910 °C, 24 h	910 °C, 24 h	450 °C, 48 h
Sm-Pr	910 °C, 24 h	910 °C, 24 h	450 °C, 48 h

Element distribution in individual 1:2:3 crystals of the sintered samples was determined in a scanning electron microscope (Jeol 820) equipped with an energy dispersive spectrometer (EDS, Link QX 200). For each composition several crystals were selected, and for each crystal more than five randomly chosen points were analyzed.

The oxygen content was determined by thermogravimetric analyses (Setaram TAG 24). The estimated accuracy is ± 0.02 in δ for the $Sm_{1-x}Pr_xBa_2Cu_3O_{7-\delta}$ samples, while for the Ca-Pr-substituted samples in Y- and Sm-based hosts, the corresponding value is somewhat larger (± 0.04) due to the presence of impurity phases.

B. Analysis of impurities

The samples of $Sm_{1-x}Pr_xBa_2Cu_3O_{7-\delta}$ were monophasic for all values of x, i.e., only reflections belonging to the orthorhombic 1:2:3 phase were observed. On the other hand, in Ca-Pr doping of the Y- and Sm-based 1:2:3 samples, impurity reflections were observed for $x \geq 0.2$ in $Sm_{1-2x}Ca_xPr_2Ba_2Cu_3O_{7-\delta}$, and $Y_{1-2x}Ca_xPr_xBa_2Cu_3O_{7-\delta}$, which could be assigned to $BaCuO_2$.

The analyses of impurities in Ca-Pr-doped 1:2:3 samples were similar in both Y- and Sm-based samples. Thus the estimated $BaCuO_2$ concentration was found to increase rapidly above about $x=0.25$ in both cases. Furthermore the element analysis of individual crystals showed that in both series the crystals contained approximately the same amount of Ca and Pr for $x \leq 0.25$, while for larger x values the Ca/Pr ratio decreases with increasing x. An example of this analysis is given in Fig. 1, where the Ca/Pr ratio and the estimated $BaCuO_2$ concentration are given as a function of nominal Ca-Pr concentration in the Y-based 1:2:3 compound. A similar graph was shown previously for Sm-based samples.[24]

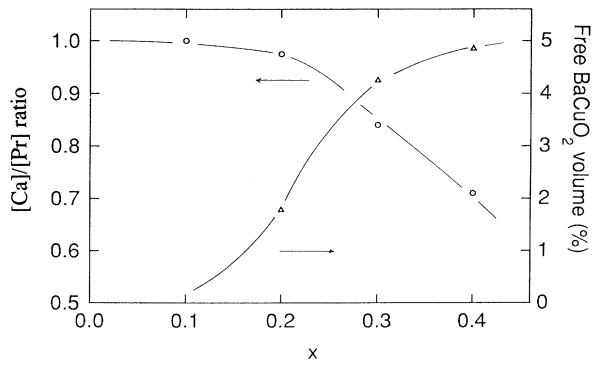

FIG. 1. Chemical analysis of $Y_{1-2x}Ca_xPr_xBa_2Cu_3O_{7-\delta}$. Left scale: ratio of Ca and Pr content in crystals; right scale: volume % of $BaCuO_2$. The curves are guides to the eye.

From the stoichiometry of the prepared powders one would therefore expect the samples with $x \geq 0.25$ to also contain some Ca-containing compound. In fact, careful examination in the scanning electron microscope of such samples showed the existence of areas in which, within experimental error, Ca was the only metal. Since the x-ray photographs did not contain any lines besides those belonging to the 1:2:3 phase or to $BaCuO_2$, it seems likely that such a Ca compound is amorphous.

C. New concentration variables z and y

We thus conclude that Ca and Pr enter the orthorhombic phase in equal proportions up to $x \approx 0.25$, while for larger x values only Pr continues to dissolve in the 1:2:3 phase. Assuming that all Pr substitutes Y, the Pr concentration z is calculated from the nominal x by $z = 0.75x/(1-x)$ for $x \geq 0.25$. Due to the possibility of a small amount of Pr substituting Ba, this may slightly overestimate z. Such partial replacement of Ba by Pr was found, e.g., by Karen *et al.*,[29] and could also be a likely interpretation of the small $BaCuO_2$ content at $x = 0.2$ in Fig. 1, and for $0.1 \leq x \leq 0.2$ in Ref. 24.

In view of these results it is convenient to describe the compositions of the samples by

$$Y_{1-y-z}Ca_yPr_zBa_2Cu_3O_{7-\delta} ,$$

and

$$Sm_{1-y-z}Ca_yPr_zBa_2Cu_3O_{7-\delta} ,$$

with $y = z$ for $z \leq 0.25$ and $y \approx 0.25$ for $z > 0.25$, with z calculated from the overall x as above.

D. Oxygen concentration

The oxygen concentration δ was found to be constant within the experimental errors for three investigated sample series. Typical results for $(z, 7-\delta)$ are (0,7.00), (0.1,6.98), (0.2,6.99), (0.3,6.97) for the Pr-doped Sm-based samples and (0,7.00), (0.1,6.92), (0.2,7.01), (0.3,6.98) for Ca-Pr-doped Sm-based series, respectively. We thus conclude that charge variations due to oxygen concentration variations are negligible.

When $YBa_2Cu_3O_{7-\delta}$ is doped with Ca there is a marked decrease in oxygen concentration,[30] which thus compensates for the decreasing metallic valency. It can be noted that a similar interpretation is not possible for the present dopings. In Sm-based hosts, the oxygen concentration is close to being constant both for Pr doping as well as for Ca-Pr doping, and cannot be simply related to either Pr^{3+} or Pr^{4+}. Similar results hold for the Y-based samples. The oxygen concentration is roughly constant from neutron-diffraction data of Pr-doped 1:2:3 compounds,[31] as well as from our chemical analyses of Ca-Pr doped samples.

E. Lattice parameters

Some lattice parameters for

$$Sm_{1-y-z}Ca_yPr_zBa_2Cu_3O_{7-\delta}$$

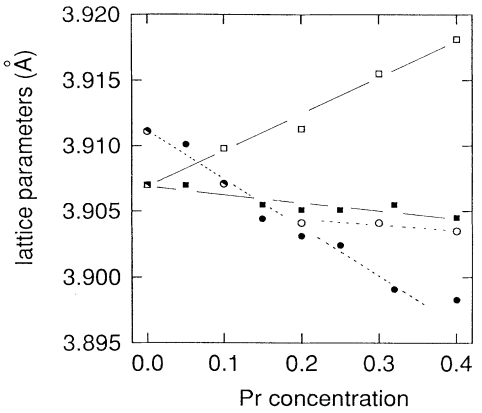

FIG. 2. The b- and c-lattice parameters of Pr- and Ca-Pr-doped Sm-based 1:2:3 samples. The full lines are guides to the eye for the b-axis data, the dotted lines for the c-axis data. ○: $c/3$ for Pr in $Sm_{1-z}Pr_zBa_2Cu_3O_{7-\delta}$; ●: $c/3$ for Ca-Pr in $Sm_{1-y-z}Ca_yPr_zBa_2Cu_3O_{7-\delta}$; □: b for Pr in $Sm_{1-z}Pr_zBa_2Cu_3O_{7-\delta}$; ■: b for Ca-Pr in $Sm_{1-y-z}Ca_yPr_zBa_2Cu_3O_{7-\delta}$. $y = z$ for $z \leq 0.25$, and $y \approx 0.25$ for $z \geq 0.25$.

and $Sm_{1-z}Pr_zBa_2Cu_3O_{7-\delta}$ are compared in Fig. 2. The c axis deceases for Pr- and Ca-Pr-doped samples at a similar rate up to $x \approx 0.2$, while for larger z values c saturates for Pr-doped samples and continues to decrease weakly for Ca-Pr doping. Since the Pr^{4+} ion (0.96 Å), in contrast to Pr^{3+} (1.126 Å), is smaller than Sm^{3+} (1.079 Å), this decreasing c-axis length might indicate a valence state of +4 for the Pr ion. However, the b axis of Pr-doped Sm-based 1:2:3 samples increases with Pr concentration, as can be seen in Fig. 2, and for the a axis (not shown in Fig. 2), the length increases both for Pr doping and, at a smaller rate, for Ca-Pr doping. The variations of lattice parameters with doping concentration therefore

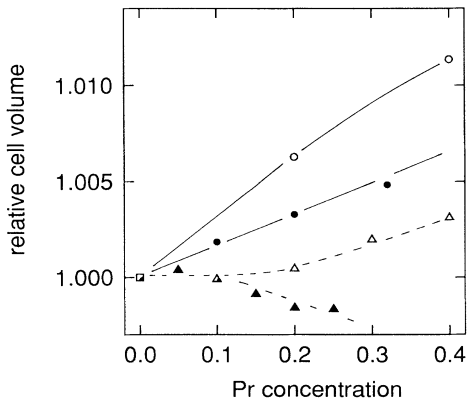

FIG. 3. Relative cell volume plotted vs Pr concentration. Circles refer to Y-based 1:2:3 samples, triangles to Sm-based 1:2:3 samples. Open symbols represent Pr doping, filled symbols Ca-Pr doping. The dashed and full lines are guides to the eye. Data for Pr in $Y_{1-z}Pr_zBa_2Cu_3O_{7-\delta}$ are from Ref. 31.

do not seem to be related in a simple way to the valency of the Pr ions, as noted previously.[23]

The relative cell volumes are plotted versus Pr concentration for the four systems in Fig. 3. For Sm-based samples the cell volume is almost constant in the cosolubility region $z \leq 0.25$ for both Pr and Ca-Pr doping. For Y-based samples the increase of the cell volume is only about half as large for Ca-Pr doping as that for Pr doping. These results show that the distortions of the unit cell due to Ca-Pr doping are small, smaller than those observed for Pr doping. This is a further indication, in addition to those discussed in Sec. IV, that Ca-Pr doping may isolate those effects of Pr doping which are not due to changes in mobile-hole concentration.

IV. T_c MEASUREMENTS AND RESULTS

A. Measurements

The cylindrical samples were cut into thin rectangular ribbons. Typical dimensions were $0.7 \times 2 \times 10$ mm^3. Four grooves were cut with a razor blade on the surface of a sample, into which thin copper wires for voltage and current leads were attached with silver paint. This arrangement gave satisfactorily low contact resistances of order 1 Ω.

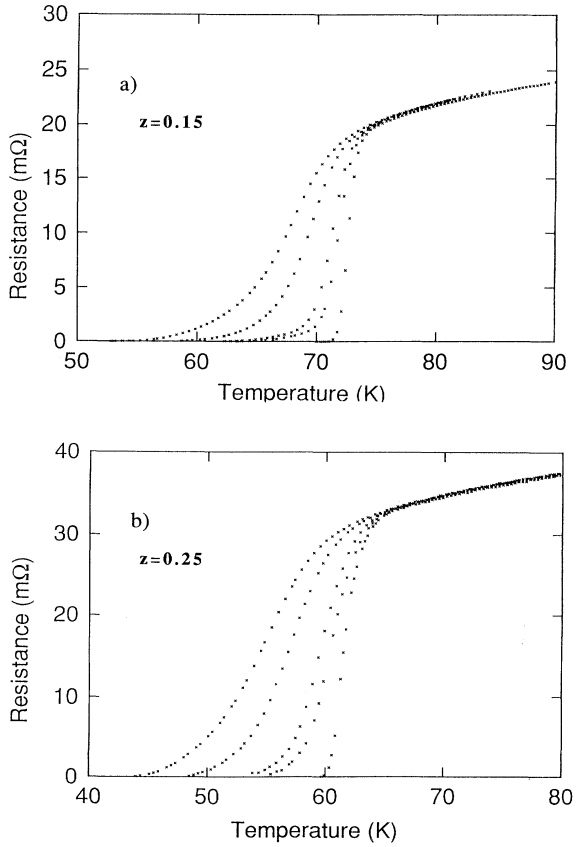

FIG. 4. (a) and (b) Examples of resistive transitions in magnetic field. Top: $Sm_{0.7}Ca_{0.15}Pr_{0.15}Ba_2Cu_3O_{7-\delta}$; bottom: $Sm_{0.5}Ca_{0.25}Pr_{0.25}Ba_2Cu_3O_{7-\delta}$; the magnetic field is 0, 0.5, 1, 4, and 8 T from right to left in both figures.

Magnetic fields up to 12 T were provided by a superconducting magnet. Platinum resistors were used as thermometers. The magnetoresistance $R(T,B)$ of these thermometers was measured at several temperatures and interpolated at intermediate temperatures. The temperature dependence of $R(B)$ is small in the present temperature range, and adequate corrections for the magnetoresistance of the thermometer were obtained by this method. Measuring currents were small, corresponding to current densities of order 0.1 A/cm^2.

As examples of primary data, the resistive transitions in magnetic fields are shown for two Ca-Pr-doped Sm-based samples in Fig. 4. For clarity only a few magnetic fields are included in the figure. As can be expected, the transitions broaden both with increasing magnetic field and with increased doping. It can also be noticed that a considerable broadening takes place already in small magnetic fields.

When comparing different samples below, we use resistive midpoints for the definitions of critical temperature and critical magnetic field H_{c2}. In the case of critical fields this procedure only gives a result which is related to the thermodynamic critical field. Nevertheless it gives a convenient estimate of the concentration dependence of the critical fields. Furthermore, as will be discussed below, the main features of this concentration dependence do not depend on which points on the transition curve are chosen, but are preserved also for other definitions of the critical magnetic field.

B. T_c

The transition temperatures are given as a function of Y and Sm concentration for Pr- and Ca-Pr-doped samples in Figs. 5(a) and 5(b). T_c is normalized to the value T_{c0} at $z=0$ for each series. The data for $Y_{1-z}Pr_zBa_2Cu_3O_{7-\delta}$ are from the magnetic measurements given in Ref. 12.

It can be seen that the addition of Ca to Pr-doped samples results in a marked increase in T_c for both hosts and for all concentrations in the cosolubility region $z \leq 0.25$. Furthermore, T_c decrease linearly with decreasing Y or Sm concentration for Ca-Pr-doped samples, in contrast to the accelerated depression for Pr-doped samples.

Figure 6 shows T_c/T_{c0} as a function of Pr concentration for all four Ca-Pr-doped sample series of Table I. There is some scatter in the data of the Y-Ca-Pr-II series, but the general linear trend is confirmed.

C. H_{c2}

The midpoint resistive transitions at different magnetic fields are shown for Pr- and Ca-Pr-doped Sm-based samples in Fig. 7. This estimate of H_{c2} is linear in temperature for magnetic fields above about 3 T for all samples. A similar conclusion was found previously also for Ca-Pr-doped Y-based 1:2:3 compounds.[23] It is interesting to note that analysis of the slightly curved region below 3 T, when plotted as H_{c2} normalized to its value at $0.9T_c$ vs T/T_c, shows that this curvature is similar to some obser-

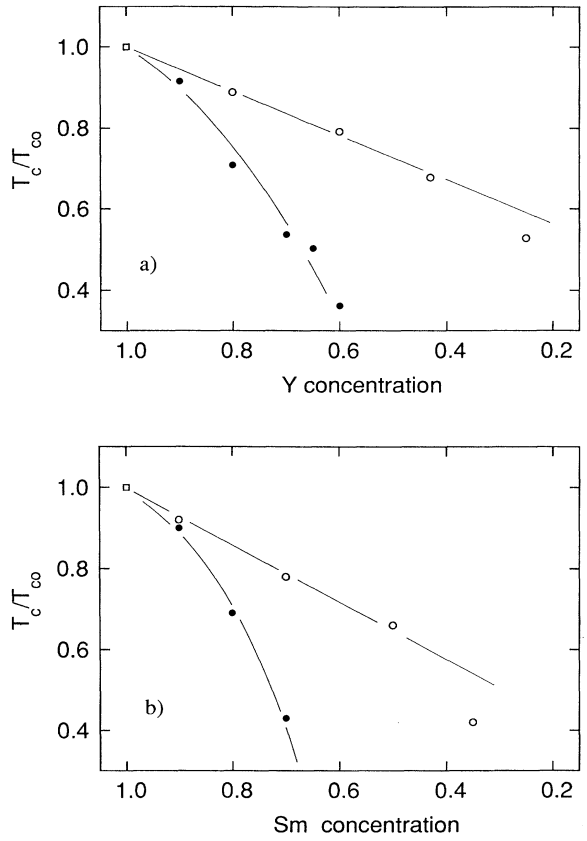

FIG. 5. (a) and (b) Reduced transition temperature plotted vs Y and Sm content. Top: ○: T_c/T_{c0} vs Y content in $Y_{1-y-z}Ca_yPr_zBa_2Cu_3O_{7-\delta}$; ●: T_c/T_{c0} vs Y content in $Y_{1-z}Pr_zBa_2Cu_3O_{7-\delta}$; bottom: ○: T_c/T_{c0} vs Sm content in $Sm_{1-y-z}Ca_yPr_zBa_2Cu_3O_{7-\delta}$; ●: T_c/T_{c0} vs Sm content in $Sm_{1-z}Pr_zBa_2Cu_3O_{7-\delta}$.

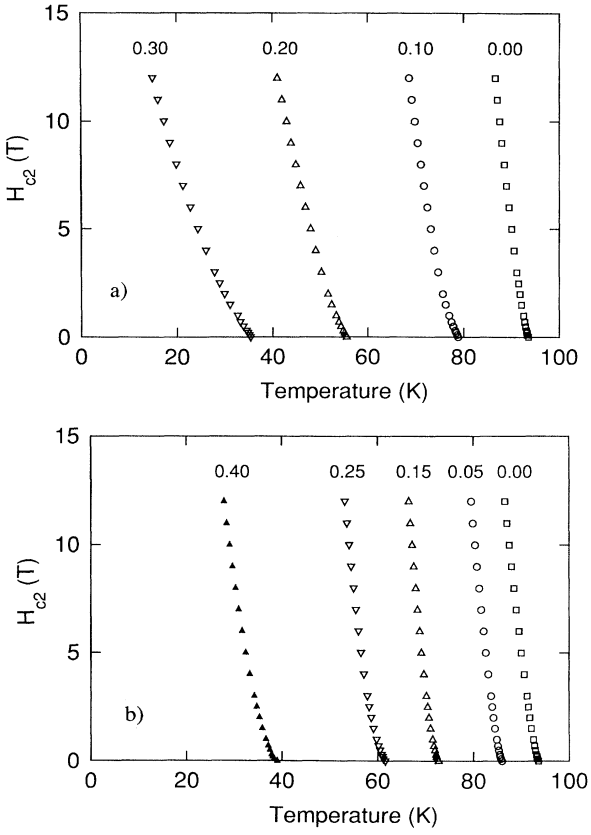

Fig. 7. $H_{c2}(T)$ for Sm-based 1:2:3 superconductors estimated from 50% of the resistive drop. Top: $Sm_{1-z}Pr_zBa_2Cu_3O_{7-\delta}$; bottom: $Sm_{1-y-z}Ca_yPr_zBa_2Cu_3O_{7-\delta}$. The appropriate z values are given above each curve.

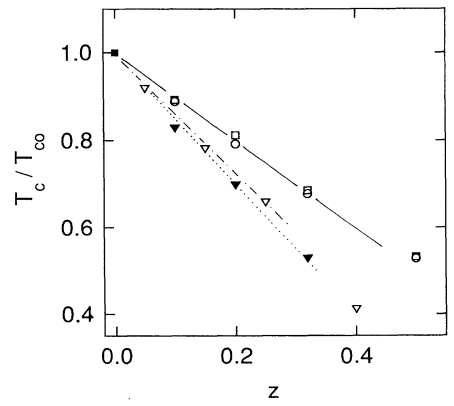

FIG. 6. T_c/T_{c0} vs Pr content in Ca-Pr-doped 1:2:3 samples. ○: $Y_{1-y-z}Ca_yPr_zBa_2Cu_3O_{7-\delta}$, Series I; □: $Y_{1-y-z}Ca_yPr_zBa_2Cu_3O_{7-\delta}$, Series II; ▽: $Sm_{1-y-z}Ca_yPr_zBa_2Cu_3O_{7-\delta}$; ▼: $Nd_{1-y-z}Ca_yPr_zBa_2Cu_3O_{7-\delta}$.

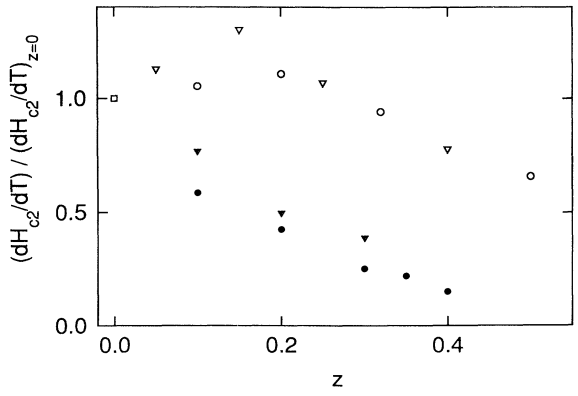

FIG. 8. Pr concentration dependence of the normalized critical magnetic field slope for four systems. Filled symbols: only Pr-doped 1:2:3 superconductors; open symbols: Ca-Pr-doped samples; circles: Y-based 1:2:3 samples; triangles: Sm-based 1:2:3 samples. (Results for $Y_{1-z}Pr_zBa_2Cu_3O_{7-\delta}$, filled circles, have been taken from magnetic data in Ref. 12.)

vations in other superconductors which also exhibit weak pinning, such as amorphous metals with T_c of below about 2 K.[32]

dH_{c2}/dT was evaluated from straight lines fitted to the data in the field range 4–12 T. The results for the concentration dependence of this slope are shown in Fig. 8. In order to allow for convenient comparison the normalized values of dH_{c2}/dT for the four different systems are given in the figure.

For the Y- and Sm-based samples which are doped with Pr only, the depression of $-dH_{c2}/dT$ with increasing Pr concentration is fairly strong and is similar in both sets of samples. These data were obtained by different methods; magnetic measurements for $Y_{1-z}Pr_zBa_2Cu_3O_{7-\delta}$ from Ref. 12, and the present resistive measurements for $Sm_{1-z}Pr_zBa_2Cu_3O_{7-\delta}$. The agreement between these two sets of data thus gives further support for our contention that resistive estimates of H_{c2} are useful for intercomparisons in a series of related samples.

In contrast to the Pr-doped samples, $-dH_{c2}/dT$ for the Ca-Pr-doped samples is almost constant, with even an apparent small increase for small z. For $z \geq 0.25$ on the other hand, $-dH_{c2}/dT$ decreases with increasing z at a rate which is comparable in both series and roughly equal to that observed for Pr-doped samples. Recalling that the cosolubility limit of Ca-Pr in the orthorhombic phase is close to $z=0.25$, we may interpret this stronger decrease of $-dH_2/dT$ at large values of z as caused by the uncompensated Pr effect in 1:2:3 superconductors.

The small increase of $-dH_{c2}/dT$ in the cosolubility region for both hosts is in qualitative agreement with the expected increased disorder scattering for increasing doping concentration, resulting in a decrease of the mean free path.

In order to check that the results for the concentration dependence of the critical magnetic field obtained from Fig. 9 did not depend on the definition of H_{c2} the analysis was repeated with H_{c2} defined as the point on the resistance R vs temperature curve which corresponds to a 10% resistivity drop. This measure of H_{c2} is probably closer to the thermodynamic critical field. The result is shown in Fig. 9. The data are more scattered here since the smaller temperature shifts in the upper region of resistance curves reduce the accuracy (see Fig. 4). Nevertheless the main features from Fig. 8 are preserved and a consistent picture of the critical magnetic field emerges; $-dH_{c2}/dT$ decreases with increasing z already for small z in $Sm_{1-z}Pr_zBa_2Cu_3O_{7-\delta}$. In the two Ca-Pr-doped systems, $-dH_{c2}/dT$ is roughly constant in the cosolubility region and decreases for larger values of z at a rate comparable to that observed in samples doped with Pr only.

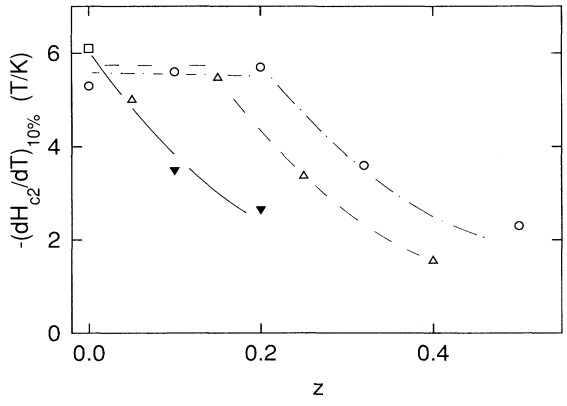

FIG. 9. Pr concentration dependence of the critical magnetic-field slope for three systems. H_{c2} is estimated from 10% of the resistive drop. ○: $Y_{1-y-z}Ca_yPr_zBa_2Cu_3O_{7-\delta}$; △: $Sm_{1-y-z}Ca_yPr_zBa_2Cu_3O_{7-\delta}$; ▼: $Sm_{1-x}Pr_zBa_2Cu_3O_{7-\delta}$. The square is the $z=0$ point for Sm-based 1:2:3 samples. The three curves are guides to the eye only.

V. DISCUSSION AND CONCLUSIONS

A. T_c

By doping 1:2:3 superconductors with equal amounts of Ca and Pr, it was seen in Fig. 5 that the strong depression of T_c due to Pr doping only was arrested and a linear decrease of T_c with doping concentration was obtained. This result indicates that we have isolated some characteristic effect of Pr, and compensated for other effects, presumably charge density variations, by also adding Ca. We will argue below that the decrease of T_c in the cosolubility region is likely of magnetic origin. It can also be noted that our result is apparently more general than the correlation between T_c depression and ionic size, which was based on doping in different 1:2:3 compounds with Pr only.[33] In that case the host $4f$ elements had to be divided into two classes depending on whether T_c vs Pr concentration was linear or not.

It can be seen in Fig. 6 that the depression of T_c at constant Ca-Pr concentration increases in the sequence Y, Sm, Nd. Straight lines were fitted to the data in the cosolubility region $x \leq 0.25$. These depression rates are plotted in Fig. 10 vs ionic radius of host atom divided by the a-axis length. The latter procedure is introduced in

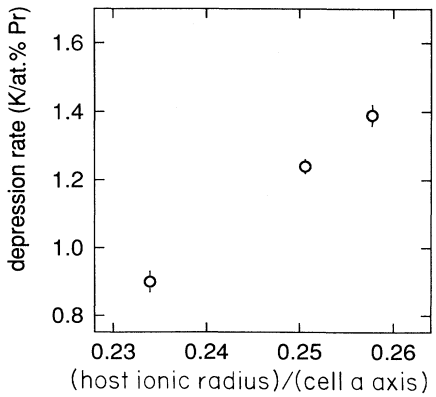

Fig. 10. The slope of the straight lines in Fig. 6 vs normalized host-ion radius (see text). The three points are from the left: Y-, Sm-, and Nd-based 1:2:3 samples, respectively, which have been doped with equal amounts of Ca and Pr. The bars are estimated errors in the fitted straight lines.

order to compensate for the increase in the a- and b-axes lengths with increasing radii of the ion at the Y position. The abscissa in Fig. 10 is thus a measure of the overlap between Y-site wave functions.

For a small concentration of paramagnetic impurities the depression of T_c is linear in impurity concentration z, and can be expressed within the AG theory as

$$T_c - T_{c0} \approx -z\frac{NJ^2}{k_B}\beta \,, \tag{1}$$

where T_{c0} is the unperturbed transition temperature, N the density of states, J the exchange interaction parameter, and β is a simple function of the impurity angular momentum.[34] It can be seen in Fig. 10 that $T_c - T_{c0}$ is of the order -1 K/at. %, which would be a rather large value for nonmagnetic substitutions in a superconducting system. Such a depression rate may therefore by itself indicate a magnetic pair-breaking effect. Of course, for high-T_c superconductors, there is the possibility that T_c is strongly sensitive to other factors which are not known.

Furthermore, it is seen in Fig. 10 that the depression of T_c increases linearly with wave-function overlap on the Y position. This may suggest that the Pr depairing effect is correlated to the size of the host ions resulting in an enhanced exchange interaction parameter for larger radius of the ions.

B. H_{c2}

The application of a magnetic field to a superconductor acts as a pair breaker. In the presence of magnetic impurities and magnetic field one must therefore consider multiple pair breaking. Assuming these to be independent, one can simply add them. If α_{cr} is the pair-breaking parameter which reduces T_c to zero we therefore write

$$\frac{\alpha}{\alpha_{cr}} = \frac{H_{c2}(T)_{z=0}}{H_{c2}(0)_{z=0}} = \left[\frac{\alpha}{\alpha_{cr}}\right]_i + \frac{H_{c2}(T)_{z>0}}{H_{c2}(0)_{z=0}} \,, \tag{2}$$

where the first equality applies to the case where the impurity concentration $z=0$, and in the right-hand member, pair-breaking parameters from impurities i and the magnetic field have been added.

In the original Abrikosov-Gorkov theory, α_i is temperature independent and proportional to $zNJ^2\beta$ of Eq. (1). It can be seen from Eq. (2) that $H_{c2}(T)$ for a doped sample then is obtained from a pure sample by subtracting a constant (the impurity pair breaking). In this case therefore the slopes of the critical-field curves are constant as a function of impurity concentration. In more general situations α_i may depend on temperature, e.g., for the reentrant superconductors α_i increases with decreasing temperature, implying from Eq. (2) that the critical-field slopes decrease with increasing impurity concentration.

Assuming that Pr in Ca-Pr-doped samples with $z<0.25$ acts as a magnetic pair breaker, we infer from Figs. 8 and 9 that the pair-breaking parameter is close to being temperature independent and apparently decreases slightly with decreasing temperatures as in weakly magnetic or pair-weakening systems.

This analysis is tentative. Resistive measurements of $H_{c2}(T)$ in high-temperature superconductors may be influenced by flux-flow effects. In fact, recent results for $Y_{1-x}Pr_xBa_2Cu_3O_{7-\delta}$ suggest that the H vs T curve obtained from resistive measurements may rather represent the irreversibility line.[35] On the other hand, our result does not depend on the point chosen on the $R(T,H)$ curves to represent $H_{c2}(T)$, as shown by the results in Figs. 8 and 9. The critical-field gradients corresponding to a 10% resistive drop are more than twice as large as those corresponding to resistive midpoints, and clearly quite different $H(T)$ curves are mapped out by these different definitions. $H_{c2}(T)$ defined as in Fig. 9 is expected to be much closer to the thermodynamic critical field than $H_{c2}(T)$ from Fig. 8, and the observation that the conclusions are similar may therefore give some empirical justification for our approach.

According to our analysis, the results thus indicate that there is no reentrant superconductivity in Pr-doped 1:2:3 superconductors. We note, however, that resistive measurements in $Y_{1-x}Pr_xBa_2Cu_3O_{7-\delta}$ at larger x values than studied here recently gave support for a temperature-dependent pair breaking with a negative exchange interaction parameter.[8] In this case a magnetic-field-induced superconducting transition could occur close the metal insulator transition in the Y-Pr 1:2:3 system. This has, however, not been observed to date.

Summarizing our results we have substituted Ca and Pr in equal proportions in different 1:2:3 superconductors and found that the cosolubility region in the orthorhombic phase extends up to about 50% substitution of the Y-site ion. By this substitution an impurity effect of Pr in 1:2:3 superconductors can be isolated as evidenced by the linear depression of T_c with Pr concentration. This depression rate is rather strong and furthermore, it increases with increasing host-ion radius. These observations suggest magnetic pair breaking by Pr ions.

The critical magnetic field gradients have different concentration dependence in samples substituted with Pr only, as compared to those with substitution of Ca and Pr. When analyzed in terms of magnetic pair breaking these data suggest that the pair-breaking parameter is almost temperature independent.

ACKNOWLEDGMENTS

Stimulating discussions with Ö. Fischer are gratefully acknowledged. This work has been supported by the Swedish Natural Science Research Council.

[1]See, e.g., H. Radousky, J. Mater. Res. **7**, 1917 (1992).
[2]Y. Dalichaouch, M. S. Torikachvili, E. A. Early, B. W. Lee, C. L. Seaman, K. N. Yang, H. Zhou, and M. B. Maple, Solid State Commun. **65**, 1001 (1988).
[3]C. H. Jee, A. Kebede, D. Nichols, J. E. Crow, T. Mihalisin, G. H. Myer, I. Perez, R. E. Salomon, and P. Schlottman, Solid State Commun. **69**, 379 (1989).
[4]D. W. Cooke, R. S. Kwok, R. L. Lichti, T. R. Adams, C. Boekema, W. K. Dawson, A. Kebede, J. Schwegeler, J. E. Crow, and T. Mihalisin, Phys. Rev. B **41**, 4801 (1990).
[5]C. L. Seaman, J. J. Neumeier, M. B. Maple, L. P. Le, G. M. Luke, B. J. Sternlieb, Y. J. Uemura, J. H. Brewer, R. Kadono, R. F. Keifl, S. R. Krietzman, and T. M. Riseman, Phys. Rev. B **42**, 6801 (1990).
[6]A. Matsuda, K. Kinoshita, T. Ishii, H. Shibata, T. Watanabe, and T. Yamada, Phys. Rev. B **38**, 2910 (1988).
[7]G. Nieva, S. Ghamaty, B. W. Lee, M. B. Maple, and I. K. Schuller, Phys. Rev. B **44**, 6999 (1991).
[8]M. B. Maple, B. W. Lee, J. J. Neumeier, G. Nieva, L. M. Paulius, and C. L. Seaman, J. Alloys Compounds **181**, 135 (1992).
[9]E. E. Alp, G. K. Chenoy, L. Soderholm, G. L. Goldman, D. G. Hinks, B. W. Veal, P. A. Montano, and D. E. Ellis, in *High-Temperature Superconductors,* edited by M. B. Brodsky, R. C. Dynes, K. Kitazawa, and H. L. Tuller, MRS Symposia Proceedings No. 99 (Materials Research Society, Pittsburgh, 1988), p. 177.
[10]F. W. Lytle, G. van der Laan, R. B. Gregor, E. M. Larson, C. E. Violet, and J. Wong, Phys. Rev. B **41**, 8955 (1990).
[11]J. Kircher, M. Cardona, S. Gopalan, H. U. Habermeier, and D. Fuchs, Phys. Rev. B **44**, 2410 (1991).
[12]J. L. Peng, P. Klavins, R. N. Shelton, H. B. Radousky, P. A. Hahn, and L. Bernadez, Phys. Rev. B **40**, 4517 (1989).
[13]See, e.g., M. B. Maple, Appl. Phys. **9**, 179 (1976).
[14]J. J. Neumeier and M. B. Maple, Physica C **191**, 158 (1992).
[15]Y. X. Jia, J. Z. Liu, M. D. Lan, P. Klavins, R. N. Shelton, and H. B. Radousky, Phys. Rev. B **45**, 10 609 (1992).
[16]G. Y. Guo and W. M. Temmerman, Phys. Rev. B **41**, 6372 (1990).
[17]J. Fink, N. Nücker, H. Romberg, M. Alexander, M. B. Maple, J. J. Neumeier, and J. W. Allen, Phys. Rev. B **42**, 4823 (1990).
[18]I. S. Yang, A. G. Schrott, and C. C. Tsuei, Phys. Rev. B **41**, 8921 (1990).
[19]I. S. Yang, G. Burns, F. H. Dacol, and C. C. Tsuei, Phys. Rev. B **42**, 4240 (1990).
[20]C. R. Fincher, Jr. and G. B. Blanchet, Phys. Rev. Lett. **67**, 2902 (1991).
[21]J. J. Neumeier, T. Björnholm, M. B. Maple, and I. K. Schuller, Phys. Rev. Lett. **63**, 2516 (1989).
[22]J. P. Franck, S. Gygax, J. Jung, M. A. Mohamed, and G. I. Sproule, in *High-Temperature Superconductivity, Physical Properties, Microscopic Theory, and Mechanisms,* edited by J. Ashkenazi, S. E. Barnes, F. Zuo, G. C. Vezzoli, and B. M. Klein (Plenum, New York, 1991), p. 411.
[23]M. Andersson, Ö. Rapp, Z. Hegedüs, T. L. Wen, and M. Nygren, Physica C **190**, 255 (1992).
[24]T. L. Wen, T. Hörlin, M. Nygren, M. Andersson, and Ö. Rapp, *Proceedings of the Moscow State University International Workshop on Chemistry and Technology of High Temperature Superconductors, Moscow, 1991,* Vol. 1, pp. 133 (1992).
[25]Y. Xu and W. Guan, Solid State Commun. **80**, 105 (1991).
[26]S. K. Malik, C. V. Tomy, and P. Bhargava, Phys. Rev. B **44**, 7042 (1991).
[27]G. Nieva, B. W. Lee, J. Guimpel, H. Iwasaki, M. B. Maple, and I. K. Schuller, Physica C **185–189**, 561 (1991).
[28]K. E. Johansson, G. Palm, and P. E. Werner, J. Phys. E **13**, 1289 (1980).
[29]P. Karen, H. Fjelvåg, O. Braten, A. Kjekshus, and H. Bratsberg, Acta Chem. Scand. **44**, 994 (1990).
[30]C. Greaves and P. R. Slater, Supercond. Sci. Technol. **2**, 5 (1989).
[31]J. J. Neumeier, T. Björnholm, M. B. Maple, J. J. Rhyne, and J. A. Gotaas, Physica C **166**, 191 (1990).
[32]See, e.g., A. Nordström, Ö. Rapp, and Z. Y. Liu, Phys. Rev. B **41**, 6708 (1990), and references therein.
[33]Y. Xu and W. Guan, Phys. Rev. B **45**, 3176 (1992).
[34]See, e.g., M. B. Maple, in *Magnetism V,* edited by H. Suhl (Academic, New York, 1973), p. 283.
[35]C. C. Almasan, M. C. de Andrado, Y. Calichaouch, J. J. Neumeier, C. L. Seaman, M. B. Maple, R. P. Guertin, M. V. Kuric, and J. C. Garland, Phys. Rev. Lett. **69**, 3812 (1992).